Enhanced performance of thin-film nanocomposite RO/NWF membrane by adding ZnO nanospheres in aqueous phase during interfacial polymerization process

Hongbin Li[*1], Wenying Shi[1], Yuheng Su[1], Hongxiang Hou[2], Qiyun Du[3],
Haixia Zhang[1] and Xiaohong Qin[1,4]

[1]*School of Textiles Engineering, Henan Engineering Laboratory of New Textiles Development,
Henan Institute of Engineering, Zhengzhou 450007, P.R. China*
[2]*Xinxiang Xinli Purification Technology Co., Ltd., Xinxiang, 453000, P.R. China*
[3]*State Key Laboratory of Hollow Fiber Membrane Materials and Processes, Tianjin Polytechnic University,
Tianjin 300387, P.R. China*
[4]*School of Textiles Science, Donghua University, Shanghai 201620, P.R. China*

Abstract. A novel thin-film nanocomposite (TFN) reverse osmosis (RO)/non-woven fabric (NWF) membrane was prepared by adding zinc oxide (ZnO) nanospheres (30 ± 10 nm) during the interfacial polymerization process of *m*-phenylenediamine (MPD) and trimesoyl chloride (TMC) on self-made polysulfone (PSF) membrane/polyester (PET) non-woven fabric support. The improved performance of TFN RO membrane was verified in terms of water contact angle (WCA), water flux, salt rejection, antifouling properties and chlorine resistance. The results showed that the WCA value of TFN RO surface had a continuous decrease with the increasing of ZnO content in MPD aqueous solution. The water flux of composite TFN RO membranes acquired a remarkable increase with a stable high solute rejection (94.5 %) in 1 $g \cdot L^{-1}$ NaCl aqueous solution under the optimized addition amount of ZnO (1 wt%). The continuous testing of membrane separation performance after the immersion in sodium hypochlorite solution indicated that the introduction of ZnO nanospheres also dramatically enhanced the antifouling properties and the chlorine resistance of composite RO membranes.

Keywords: nanocomposite membrane; reverse osmosis; hydrophilicity; antifouling properties; chlorine resistance

1. Introduction

With the rapid development of the global economy and the acceleration of urbanization, the demand for freshwater resources becomes increasingly urgent. In contrast, the environmental pollution and the excessive exploitation result in the serious shortage of freshwater resources and affect the economic and social developments especially in many developing contries. As the most

---

∗Corresponding author, Ph.D., E-mail: lihongbinnn@163.com

important technology for desalination, reverse osmosis (RO) has been widely used to produce freshwater from saline water and other wastewater sources (Ni *et al*. 2014). So far, most commercially available RO membranes are aromatic polyamide (PA) thin-film composite (TFC) types which were prepared via interfacial polymerization.

TFC aromatic PA RO membranes have a multilayer structure which is commonly composed of the nonwoven fabric bottom layer, porous support membrane and the PA top layer. This structure can be independently optimized and thus endows membrane with superior separation performance including water flux and salt rejection, resistance to pressure compaction and wide pH range (Gu *et al*. 2015, Yan *et al*. 2016). However, two major challenges in practical application of TFC RO membranes are membrane fouling and the chlorine vulnerability. The deposition and absorption of solute or particles from feeding water onto RO membrane surface and into pores induce membrane fouling. The mechanisms of RO membrane fouling can be categorized into four types: minerals, organic matters, colloidal and biological substance. Among them, the foling of biological substance is the major cause of RO fouling (Al-Juboori and Yusaf 2012). The serious membrane fouling can cause the flux decline and deteriorate the quality of the permeation water. Although the performance of fouled RO membranes can be partially recoved after the backflushing and chemical cleaning, it would also suffer inevitable flux decline especially after long-term fouling. Consequently, the operation difficulty and cost would increase.

The fouling resistance of RO membrane could be improved through the surface grafting of hydrophilic polymers such as triethylene glycol dimethyl ether (triglyme) (Zou *et al*. 2011), the zwitterionic carbox- ybetaine methacrylate (CBMA) (Wang *et al*. 2015), and polyvinyl alcohol (PVA) (Liu *et al*. 2015), or through the coating of hydrophilic matters such as polydopamine (Karkhanechi *et al*. 2014), poly(N-vinylpyrrolidone) (PVP) (Wu *et al*. 2015), amino acid 3-(3,4-dihydroxyphenyl)-l-alanine (l-DOPA) (Azari *et al*. 2014), etc. Besides, the layer-by-layer (LbL) deposition technique has been successful used to improve membrane's fouling resistance. Poly(ethylene glycol) (PEG) acrylate multilayers in the nanometer range could be assembled via the layer-by-layer (LbL) deposition technique on polyamide RO membrane surface and stabilized using click chemistry (Wang *et al*. 2012). The resistance to fouling of the novel RO membrane increased as the number of PEG bilayers was increased. The flux of the fouled modified RO membrane fell only 9-17% due to the presence of the multilayer coating. In addition, Choi (Choi *et al*. 2013) coated graphene oxide (GO) multilayers on the PA TFC membrane surface via LbL deposition technique and found that the novel RO membrane possessed improved resistance to fouling which was mainly due to the improved surface hydrophilicity.

RO membrane's chlorine resistance mainly depends on the polymer's nature. Compared with the cellulose acetate asymmetric RO membranes, polyamide TFC RO membranes are more sensitive to chlorine (Hong *et al*. 2013). The chlorine-sensitive sites in the PA layer such as the amide nitrogen and the aromatic ring associated with amine are vulnerable to the chlorine attack which induces the degradation of polyamide chains and sharply deteriorated membrane separation performance (Glater *et al*. 1994). Much effort has been made to develop novel membranes with better chlorine tolerances or to improve the chlorine resistance of polyamide TFC membranes through the surface coating, surface grafting or blending.

The development of novel RO membranes with better chlorine tolerances is mainly centered on the exploration of new monomers for the interfacial polymerization. Shintani *et al*. (2007) selected the *N*, *N'*-dimethyl-m-phenylenediamine (*N*, *N'*-DMMPD) and 1, 3, 5-benzenetricarbonyl trichloride (TMC) as the aqueous and organic phase monomers, respectively. The novel RO membrane showed much higher chlorine resistance than commercial polyamide and cellulose

acetate RO membranes. Yu *et al*. (2009) developed a novel aromatic-cycloaliphatic polyamide TFC RO membrane with improved chlorine resistance as well as good RO performance through the interfacial polymerization of *m*-phenylenediamine-4-methyl (MMPD) and cyclohexane-1, 3, 5-tricarbonyl chloride (HTC) on PSF support membrane. The experimental results revealed that the novel RO membrane exhibited higher chlorine resistance and better-matched water flux than that prepared from *m*-phenylenediamine (MPD) and trimesoyl chloride (TMC) at the expense of some salt rejection. The improved chlorine resistance is attributed to the reduced probability of N-chlorination and Orton-rearrangement by using monomer MMPD. Hong *et al*. (2013) prepared the chlorine-resistant polyimide TFC RO membranes via interfacial polymerization of *m*-phenylene diamine (MPD) and 1, 2, 4, 5-benzene tetracarbonyl chloride (BTC) and subsequent thermal imidization. The improved chlorine resistance is due to the elimination of chlorine-sensitive sites by the replacement of amide linkage with imide linkage.

The surface coating is a simple modification method, but the weak adhesion between the modifier and the polyamide layer is an urgent problem to be solved. Some modifiers such as silane (Kim *et al*. 2013, Shin *et al*. 2011), poly(methylacryloxyethyldimethyl benzyl ammonium chloride-r-acrylamide-r-2- hydroxyethyl methacrylate) (P(MDBAC-r-Am-r-HEMA)) (Ni *et al*. 2014) have been coated on TFC RO membrane surface and the membrane's chlorine resistance has been enhanced. Active groups can be introduced into the possible grafting sites in polyamide chains through the surface grafting method. The possible grafting sites include the amino hydrogen, the amine hydrogen associated with aromatic ring, hydrogen in carboxyl groups, and the unreacted acyl chloride groups (Cheng *et al*. 2013). A few polymers such as salicylaldehyde (SA) (Zhang *et al*. 2014), polyvinyl alcohol (PVA) (Liu *et al*. 2015), 3-monomethylol-5, 5-dimethylhydantoin (MDMH) (Wei *et al*. 2010a), 3-allyl-5,5-dimethylhydantoin (ADMH) (Wei *et al*. 2010b), crosslinked 3-allyl-5,5-dimethylhydantoin (ADMH) (Zhang *et al*. 2013), N-isopropylacrylamide (NIPAm) (Cheng *et al*. 2013), and imidazolidinyl urea (IU) (Xu *et al*. 2013) acting as the chlorine-consumer or chlorine-shielder have been successfully grafted on the active sites in polyamide chains and the chlorine resistance of the resultant RO membrane are effectively improved.

The blending of functional particles or polymers is believed to be a simple and effective modification method to improve the RO membrane's chlorine resistance. Safarpour (Safarpour *et al*. 2015) prepared a novel thin-film nanocomposite (TFN) reverse osmosis (RO) membrane by interfacial polymerization of *m*-phenylenediamine (MPD) and trimesoyl chloride (TMC) monomers. Before the interfacial polymerization, the reduced graphene oxide (rGO)/TiO_2 nanocomposite was added into the MPD solution. The chlorination tests suggested that the NaCl rejection of the bare RO membrane decreased by 30% while this value was only 3% for the TFN RO membrane. The enhanced chlorine resistance of the rGO/TiO_2/RO membranes was attributed to the improved hydrophilicity and rGO/TiO_2 barrier which is able to protect the polyamide thin layer. Moreover, the intermolecular hydrogen bonding could be strengthened due to the chemical interaction between the rGO/TiO_2 and polyamide chains and this inhibited the substitution of hydrogen with chlorine on the amide groups of the aromatic polyamide membranes. In addition to TiO_2, the pure graphene oxide (Chae *et al*. 2015) and organosilica (Yamamoto *et al*. 2015) were also successfully used to modied RO membrane's chlorine resistance.

The metallic oxide nanospheres have many superior characteristics such as UV shielding material, odor removal, antioxidant capacity and antibacterial agent. In addition, the metallic oxide with electronic effect can protect the polyamide layer away from the electrophilic chlorine attack. Among the metallic oxide nanospheres, titania (TiO_2) and its derivative are usually used in the

form of nanoparticles to improve permeate water flux and antifouling properties of composite nanofiltration membrane (Cai *et al*. 2015, Bai *et al*. 2013, Rajaeian *et al*. 2013, Peyravi *et al*. 2014). Rajaeian *et al*. (2013) prepared thin-film nanocomposite nanofiltration membrane via interfacial incorporation of aminosilanized TiO$_2$ nanoparticles. Functionalized TiO$_2$ nanoparticles were incorporated into trimesoyl chloride (TMC) organic phase. The functionalized TiO$_2$ nanoparticles improved membrane salt rejection to 54% as well as water flux to 12.3 l/m^2 h. Bai *et al*. (2013) incorporated TiO$_2$ nanoparticles in aqueous phase and prepared composite NF membrane using TMC in n-hexane as organic phase. At the optimal preparation conditions, the NF membrane showed high flux, high dye rejection and low salt rejection, which are suitable to the process of purifying raw dye.

Zinc oxide (ZnO) nanosphere has many superior characteristics of metallic oxide nanospheres such as UV shielding, odor removal, antioxidant and antibacterial capacity. Besides, zinc atom has ceiling electronic effect. Thus the incorporation of ZnO nanosphere in membrane matrix can effectively shield the polyamide layer away from the electrophilic chlorine attack and prolong membrane service life. So far, few studies have been investigated on the preparation of ZnO-incorporated composite membrane. In this study, thin- film nanocomposite (TFN) reverse osmosis (RO) membranes were prepared through the introduction of zinc oxide into aromatic polyamide layer using the polysulfone (PSF) support membrane/nonwoven fabric as the substrates. SEM, FTIR and XRD were used to characterize surface chemical structure of the resultant RO membranes. Dynamic water contact angle (WCA) was measured to investigate the hydrophilicity of membrane surface. RO membrane performance including the separation performance, antifouling properties and the resistance to chlorine were analyzed to evaluate the effects of the addition of nano zinc oxide.

2. Experimental

2.1 Materials

Trimesoyl chloride (TMC, ≥99%) and *m*-phenylenediamine (MPD, ≥99%) were obtained from Sinopharm Chemical Reagent without further purification. Polysulfone (PSF) (Solvay, Udel-3500) was dried in a vacuum oven at 80℃ for 12 h before use. Dimethylacetamide (DMAc), polyethylene glycol (PEG, M_W=6 000), sodium chloride (NaCl) and *n*-hexane were all analytical reagents purchased from Tianjin Kemiou reagent Co., Ltd. (China). Bovine serum albumin (BSA) and zinc oxide nanospheres (30±10 nm) were supplied by Aladdin Industrial Corporation (Shanghai, China). PET spunbonded NWF with the grammage of 75 g·m^{-2} was supplied from the Shijiazhuang Tianlue Advanced Textile CO. LTD.

2.2 Preparation of PSF/PET non-woven fabric support

PSF/PET non-woven fabric (NWF) support was prepared through the scrape coating technique. PSF support membrane was formed on the surface of PET non-woven fabric (NWF) support via the immersion precipitation phase inversion process. The schematic diagram of the preparation of PSF/PET NWF support was illustrated in Fig. 1. Certain amount of PSF granules (17 wt%) and compound additives (PEG-6 000, 6 wt%; LiCl, 1 wt %) were fully mixed in DMAc (76 w%) and stayed at 60℃ for 12 h until a homogeneous solution was formed. Then, the solution was vacuum
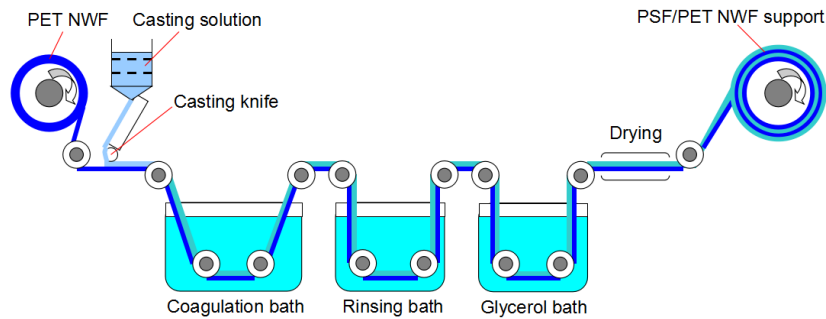
Fig. 1 The schematic diagram of the preparation of PSF/PET NWF support
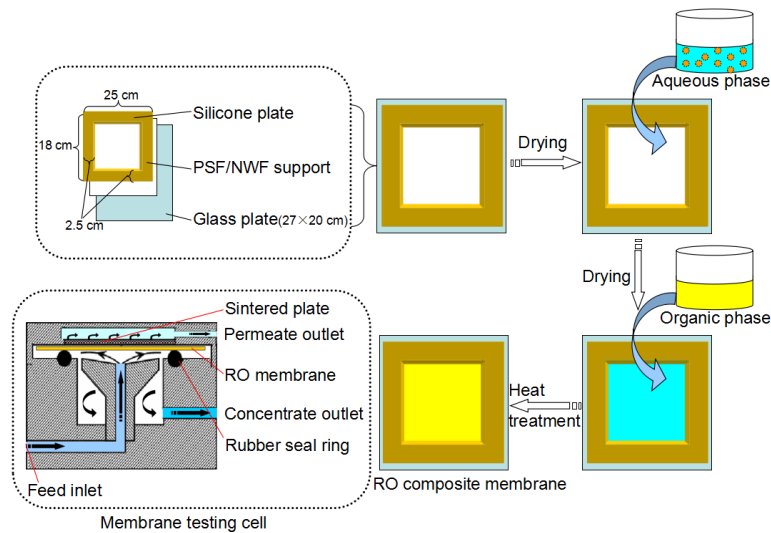

Fig. 2 The preparation flow scheme of RO composite membrane and the configuration of membrane testing cell

degassed at 30°C for 12 h and the casting solution for scrape coating was obtained. The breadth of PET NWF was 280 mm and PET NWF was soaked in ethanol and washed with pure water before use. The PET NWF wound on the running roller was transmitted to the bottom of the casting knife at a certain rate. The solution flew from the gap (100 μm) between the casting knife and the NWF surface and was evenly coated on the NWF surface. The nascent PSF support membrane was immediately formed while immersing in the water coagulation bath. Afterwards, the nascent PSF/NWF support was washed and surface treated in the rinsing bath and the glycerol bath, respectively. Finally, the PSF/NWF support was obtained after the air drying in a horizontal heated column.

2.3 Preparation of TFN RO membrane

Thin-film nanocomposite (TFN) RO membrane was prepared via the immersion coating method as illustrated in Fig. 2. 0.5 wt% MPD aqueous solution and 0.44 wt% TMC in *n*-heptane

were used as the aqueous phase and the organic phase solution, respectively. Certain amount of ZnO nanospheres were added in MPD aqueous solution and dispersed via ultrasonicating for 30 min before use. The immersion coating module was composed of the silicone plate and glass plate with the support membrane placed intermediately as shown in Fig. 2. The size of glass plate and silicone plate is 27×20 cm and 25×18 cm, respectively. And the width silicone frame is 2.5 cm. Firstly, blend MPD aqueous solution with different concentration ZnO nanospheres was poured on the top surface of the dried PSF/NWF support for 3 min. Then, the coating liquid was poured out from support membrane surface and the coating module was immediately put into the environmental chamber for 1 h at constant temperature and humidity of 30℃ and 40%. Afterwards, the organic phase solution rapidly poured onto the substrate top surface to form polyamide layer through the interfacial polymerization between MPD and TMC. The reaction was kept for 30 s and the nascent composite RO membrane was instantly put into the environmental chamber for 30 min to allow the *n*-hexane to evaporate. Subsequently, the RO membrane was post-treated to enhance the stability of functional layer structure. Finally, the resultant RO membrane was washed with pure water and stored in pure water for use. The TFN RO membranes prepared with different ZnO content in aqueous (0, 0.5, 1, 1.5, 2 wt%) were designated as RO1, RO2, RO3, RO4 and RO5, respectively.

2.4 Characterization of PSF/NWF support membrane

The porosity (ε) of PSF/NWF support membrane was defined as the ratio of pore volume to membrane geometrical volume and calculated via Eq. (1)

$$\varepsilon = \frac{(W_w - W_d)}{Al\rho} \times 100\% \tag{1}$$

where W_w and W_d were the weights of wet and dry membranes (g), respectively. A, L, and ρ were the effective area (cm^2), average thickness (cm) and deionized water density at atmosphere temperature (g·cm^{-3}).

The pore size distribution of PSF/NMF support membrane was measured through the mercury porosimetery apparatus PM33GT-17 (Quantachrome, USA).

2.5 Characterization of membrane structure and morphologies

Chemical structure of membranes was characterized by Fourier transform infrared spectra (FTIR) through a FTIR TENSOR 37 (BRUKER Corporation, Germany) in a wave number of 4000-500 cm^{-1}. All the samples were dried thoroughly in vacuum at 60℃ for 24 h prior to the characterization. Scanning electron microscopy (SEM, FEI Quanta 250, USA) was used to observe the surface morphologies of the composite RO membranes while Energy Dispersive X-Ray Spectroscopy (EDX) instruments were also used to analyze membrane surface chemical compositions. Membrane samples were freeze-dried for 24 h and sputtered with gold before SEM observation. The changes of crystal structures in the polyamide layer were examined through the X-ray diffraction (XRD, Rigaku, D/MAX-2500, Japan) with a scanning range (2θ) from 10° to 45° at a scanning speed of 2 °/min.

Water contact angle measurements were performed to evaluate the wetting ability of membrane surface using a Kruss Instrument (CM3250-DS3210, Germany) at ambient temperature. An

automatic piston syringe was used to place a water droplet of 3 μL onto membrane surface while the images were captured by a camera. At least three readings at different locations on each sample surface were obtained to get a reliable value.

2.6 RO membrane separation performance characterization

The separation performance of TFN RO membranes were measured through a cross-flow filtration of 1 g$\cdot$L^{-1} NaCl aqueous solution at 25°C under 0.7 MPa. The configuration of membrane testing cell equipped in the cross-flow system was illustrated in Fig. 2. This configuration provided sufficient contact area between the RO membrane and feed liquid, and can make the feed pressure exert uniformly on RO membrane surface. Different membrane samples were pre-pressured with pure water at 0.75 MPa to reach a stable performance before testing.

Membrane water flux (F) was obtained as

$$F = \frac{V}{A \cdot t} \tag{2}$$

F-water flux (L$\cdot$m$^{-2}\cdot$h^{-1}); V-water permeation volume (L); A-the effective membrane area (m^2), t-filtration time (h).

Salt rejection (R) was calculated as

$$R = (1 - \frac{C_p}{C_f}) \times 100\% \tag{3}$$

where C_p and C_f were the salt concentrations of the permeate and the feed liquid, respectively. The salt concentrations were examined at appropriate intervals via a conductivity meter (DDS-11A, Shanghai Leici Instrument Works, China).

The separation performance of PSF/NWF support membrane was also tested through the cross-flow filtration and the water flux was calculated via Eq. (1). The rejection of bovine serum albumin (BSA) was examined through the difference between the absorbance of the feed and permeate liquid at 510 nm using the ultraviolet-visible spectrophotometer (752, Shanghai XP-Spectrum, CO. LTD)

2.7 Membrane antifouling experiments

Membrane antifouling experiments were implemented through a three-cycle cross-flow filtration of BSA solution under 0.7 MPa at 25°C. The membrane filtration cell used had an effective membrane area of 33.2 cm^2. Water flux data were collected at an interval of 10 min during the whole filtration process. For the first filtration cycle, the data of pure water flux were measured. Then, during the second cycle, the feed was replaced by 1 g$\cdot$L^{-1} BSA phosphate buffer solution (PBS, 0.01mol$\cdot$L^{-1}, pH=7.4) and the data of water flux of BSA solution was measured. Subsequently, membranes were flushed through pure water for 30 min. Afterwards, pure water flux instead of BSA solution was used and the flux data were also collected during the third cycle. The normalized flux was employed to evaluate the flux variation which was equal to the ratio of the water flux during the whole filtration process and pure water flux in the first cycle. In addition, the flux recovery ratio which was equal to the ratio of the water flux after each washing step and pure water flux before BSA fouling in the first cycle was used to characterize the flux recovery capacity.

2.8 Membrane chlorination experiments

Chlorine resistances of the pristine and the TFN RO membranes were evaluated as follows. Firstly, different RO membranes were immersed in the 100 ppm NaClO aqueous solutions (pH=6.5) and the NaClO solution was replaced every three days. Then, membrane samples were taken out and rinsed with pure water. The water flux and NaCl rejection of the virgin RO membrane and the TFN RO membrane were measured and calculated as mentioned above to evaluate the difference of the chlorine resistance. To make the comparison more straightforward, data of the salt rejection and water flux after the chlorine exposure in this study were normalized.

3. Results and discussion

3.1 Structure parameter of PSF/NWF support membrane

The pore size distribution of PSF/NWF support membrane was shown in Fig. 3. The pore diameter mainly distributed from 250 to 550 nm which was a typical pore size range of the support membrane. The pore size distribution was relative narrow which would be favor for the adhesion of the coating layer on support membrane surface and thus obtained a high-performance RO composite membrane. Other structure parameters of PSF/NWF support membrane including the porosity, pure water flux, BSA rejection and thickness were also listed in Table 1. It could be seen
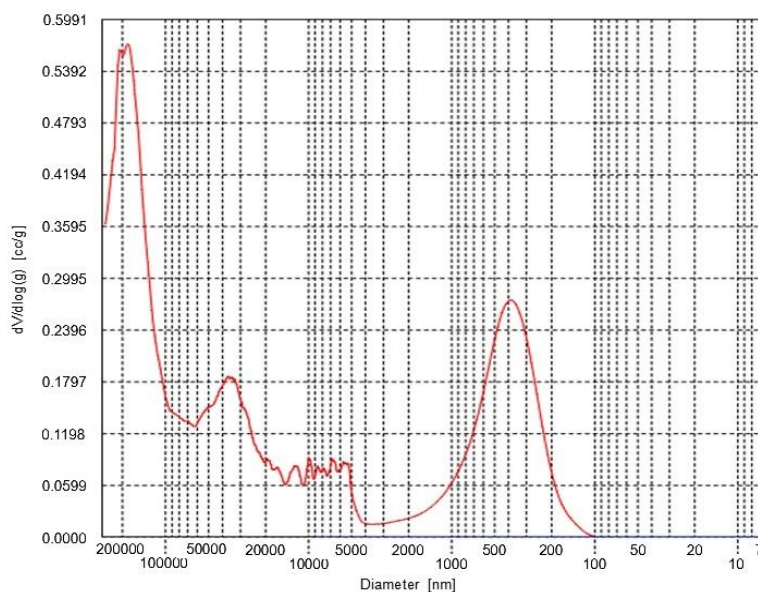

Fig. 3 Pore size distribution of PSF/NWF support membrane

Table 1 Structure parameters of PSF support membrane

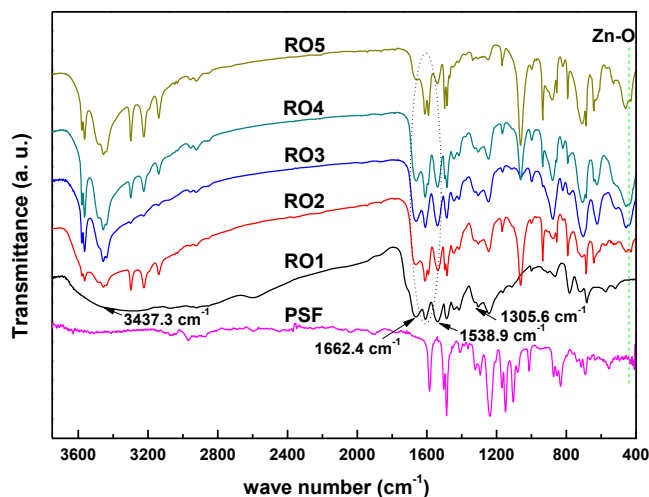| Parameter	BSA rejection (%)	Pure water flux ($L \cdot m^{-2} \cdot h^{-1}$)	Porosity (%)	Thickness (μm)
PSF/NWF support	99.2	91.6	63.8	161.2

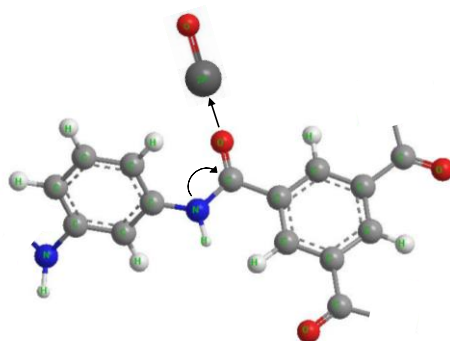Fig. 4 FTIR spectra of different membranes

Fig. 5 Illustration of the interaction between C=O groups in polyamide chains and ZnO nanospheres

that the PSF/NWF support had a high BSA rejection, high pure water flux, relative modest porosity and thickness.

The pure water flux and BSA rejection were tested under 0.1 MPa at 25℃.

3.2 Surface chemical compositions of different membranes

The ATR-FTIR spectra of different RO membrane surface were shown in Fig. 4. Compared with the PSF spectrum, the spectra of the original and TFN RO membrane (RO1) surface appeared new peaks at 1662.8, 1538.9 and 1305.6 cm^{-1}, which were attributed to the stretching vibration of the C=O bands of an amide group (amide I), amide II band for the N-H in plane bending and C-N stretching of carboxylic acids, respectively. Besides, a broad adsorption band at 3437.3 cm^{-1} was belonged to the N-H stretching vibration. These results confirmed that the polyamide layer was successfully formed on the porous PSF support membrane surface after the interfacial polymerization between MPD and TMC (IP) (Fathizadeh *et al*. 2011, Baroña *et al*. 2012). An obvious peak at 437.3 cm^{-1} ascribed to the stretching frequency of Zn-O bond emerged in all the curves of the TFN RO membranes (Stan *et al*. 2015). This result suggested the successful

introduction of ZnO nanospheres into the polyamide layer. In addition, through careful observation, the stretching vibration peak of C=O bands showed a red shift from 1662.8 in RO1 to 1653.8 cm^{-1} in RO5. This phenomenon could be attributed to the interaction between C=O groups in polyamide chains and ZnO nanospheres as illustrated in Fig. 5. Due to the electron withdrawing effect of the carbonyl groups with negative charge and the positive effect of zinc atom, these results contributes to the mutual attraction of C=O groups in polyamide chains and ZnO nanospheres

3.3 Surface morphology of composite RO membrane

Fig. 6 showed the surface morphologies of different membranes. It could be seen that PSF membrane surface exhibited a few micropores (a) which would be facilited for the adhesion of the coating layer and the preparation of high-performance RO composite membrane. The porous top surface of PSF support membrane was densely covered with the typical nodular structure and some dish-like bulges (b). This result indicated that the polyamide layer was successfully formed through the interfacial polymerization and pore sizes of the resultant membranes were in the range of reverse osmosis (Yan *et al*. 2015, Bera *et al*. 2015). With the introduction of zinc oxide (ZnO) nanospheres, the nodules grew bigger and membrane surface roughness obviously increased (c). The increased roughness promoted the increasing of membrane effective filtration area and the enhancement of RO membrane water flux (Lee *et al*. 2008). No obvious ZnO spheres could be observed in Fig. 6(c) which indicated the ZnO nanospheres were uniformly dispersed in functionally layer matrix. This result was probably due to the interaction between C=O groups in
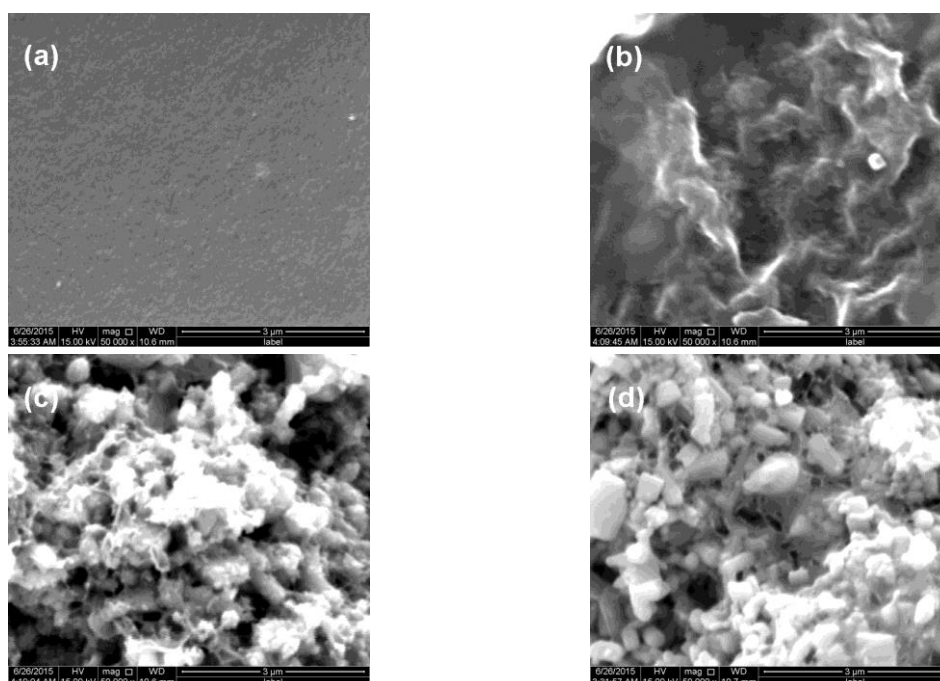

Fig. 6 SEM images of different membrane surface (a) PSF support membrane; (b) RO1; (c) RO3; (d) RO5
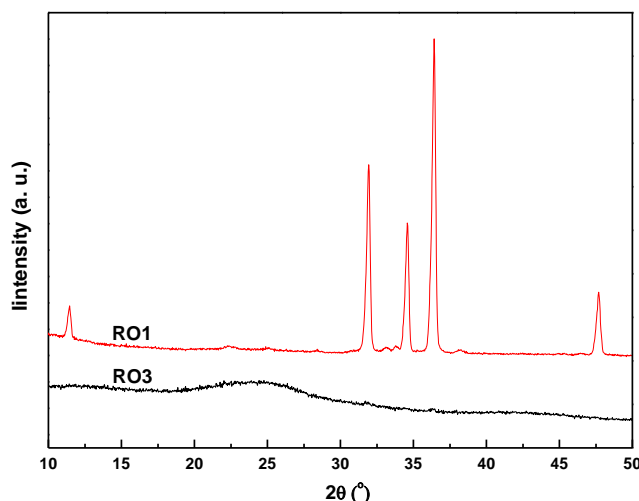
Fig. 7 X-ray diffractograms of different NF membranes

polyamide chains with the ZnO nanospheres. With the increase of ZnO amount, the aggregation of nanoparticles would get more and more serious.

3.4 Crystal structure of functional layer

Fig. 7 showed the XRD curves of the different RO membrane. Compared with original RO membrane, four obvious peaks emerged at 2θ of about 31.6°, 34.6°, 36.3° and 47.4° which were the characteristic peaks of ZnO (Stan *et al*. 2015). Different crystalline phase would change membrane separation performance (Cai *et al*. 2015, Pourjafar *et al*. 2013). Cai *et al*. (2015) pointed that the the restrictions of TiO_2 grain growth and A to R transformation reduced the pure water flux of TiO_2 membranes. It could be obtained from the measurement of membrane separation performance that the crystalline phase of ZnO nanospheres used in this study favored the separation performance improvement of RO membrane. After continuous measurement of separation performance for 48 h, the peak type and intensity in XRD curves of RO3 had nearly no change which indicated the ZnO nanospheres with moderate addition could be firmly embedded in polyamide layer. This result would be due to the combination between the C=O groups in polyamide chain and and the ZnO as analyzed in FIIR above.

3.5. Hydrophilicity of membrane surface

Membrane surface hydrophilicity has important effect on membrane permeability (Ni *et al*. 2014, Hurwitz *et al*. 2010) and is commonly characterized through the water contact angle (WCA) measurement. The dynamic WCA of different RO membrane surface was obtained in this study. As shown in Fig. 8, the initial WCA of RO3 was much lower and the dynamic WCA of RO3 decreased more rapid than that of RO1. The WCA values of RO1 at 30 s were 52.0°, whereas the value of RO3 decreased to 43.7°. These results suggested that the TFN membrane had improved wettability and hydrophilicity. The material surface roughness and intrinsic wettability of the material itself are the two main major factors affecting the WCA value (Liu *et al*. 2012, Gao *et al*.
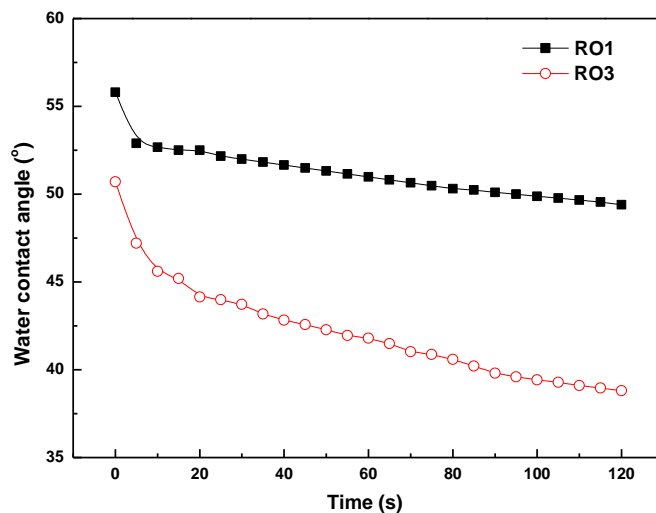
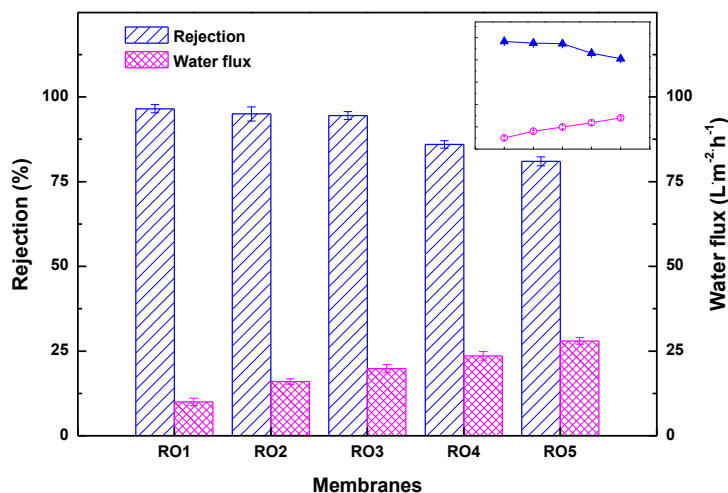Fig. 8 Dynamic water contact angle of different NF membrane

Fig. 9 Salt rejection and water flux of the virgin and modified RO membranes tested with 1 g·L^{-1} NaCl aqueous solution at 25℃ and 0.7 MPa

2013). The migration of hydrophilic nanospheres onto polyamide layer surface and the increased surface roughness as seen from the SEM images above favored the improvement of membrane surface hydrophilicity, which was essential for the enhancement of membrane permeability.

3.6 Separation performance of the TFN RO membranes

The changes of membrane structure would affect membrane performance. Fig. 9 showed the variations of salt rejection and permeation flux of the virgin and modified RO membranes tested through the cross flow filtration of 1 g·L^{-1} NaCl solution at 25℃ and 0.7 MPa. It could be seen that TFN RO membranes exhibited almost unchanged NaCl rejection and enhanced water flux when

Table 2 Separation performance of various RO membranes

Code	Functional material	Modified method	Rejection (%)	Water flux (L·m^{-2}·h^{-1})	NaCl concentration (ppm)	Testing pressure (bar)	Ref.
a	MPD/BTC-TMC	New monomer	98.8	18.8	2000	15	(Hong *et al.* 2013)
b	SiO$_2$-MPD/TMC	Nanosphere incorporation	95.6	51.3	2000	16	(Bao *et al.* 2013)
c	MPD/TMC	New support	93.8	48	2000	30	(Gorgojo and Jimenez-Solomon 2014)
d	SiO$_2$-MPD/TMC	Nanosphere incorporation	91.2	48.9	11000	44	(Peyki *et al.* 2015)
e	BaSO$_4$-MPD/TMC	Surface coating	98.4	30.5	500	5	(Zhou *et al.* 2014)
f	Ce(IV)-PVA-MPD/TMC	Surface grafting	94.0	62.9	2000	17.2	(Rana *et al.* 2015)
g	MeO-PEG-MPD -MPD/TMC	New monomer	93.0	38	2000	14	(Liu *t al.* 2015)
h	Fumed silica/CA/PEG-200	Homogeneous membrane	98.4	2.64	3500	4	(Sabir *et al.* 2015a)
i	PVA-MPD/TMC	Surface grafting	98.9	28.6	500	5	(Liu *et al.* 2015)
j	Ag-MPD/TMC	Nanosphere incorporation	98.3	55.2	2922	27.6	(Ben-Sasson *et al.* 2014)
k	Cu/polyamide	Nanosphere incorporation	94.3	41.4	2922	27.6	(Ma *et al.* 2016)
l	MWCNTs-CA/PEG 400	Homogeneous membrane	76	1.68	1000	4	(Cheng *et al.* 2013)
m	PVA-PHMG /polyamide	Surface coating	98.2	67	584	27.6	(Nikkola *et al.* 2013)
n	PA-g-NIPAm/polyamide	Surface grafting	97.6	35.5	500	5	(Cheng *et al.* 2013)
o	GO-MPD/TMC	Nanosphere incorporation	99.3	16.3	2000	27.6	(Chae *et al.* 2015)
p	Sericin/polyamide	Surface coating	98.2	28.3	500	5	(Yu *et al.* 2013)
q	ZnO-MPD/TMC	Nanosphere incorporation	94.5	21.2	1000	7	This work

the concentration of ZnO nanosphere in the aqueous phase was lower than 1 wt%. However, the NaCl rejection of TFN RO membrane showed an obvious decline and the water flux continuously increased. These results were essentially attributed to the variation of microstructure and surface properties of the functional layer. The formation of the loose functional layer and the hydrophilicity improvement of NF membrane surface after the addition of ZnO nanospheres favored the obvious increasing of water flux. When the ZnO content increased over 1 wt%, the larger void space emerged among the polyamide network and induced the apparent decline of salt
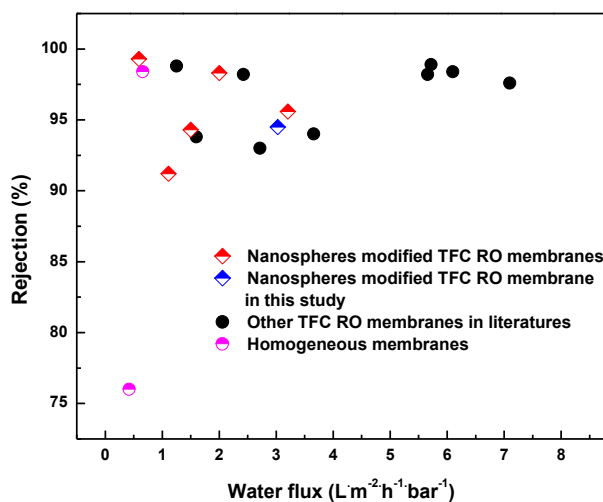
Fig. 10 Relationship between water flux and NaCl rejection of various RO membranes

rejection.

Table 2 summarized the separation performance of various RO membranes obtained in this work and reported in previous literatures (Liu *et al*. 2015, Hong *et al*. 2013, Cheng *et al*. 2013, Chae *et al*. 2015, Bera *et al*. 2015, Bao *et al*. 2013, Gorgojo and Jimenez-Solomon, 2014, Peyki *et al*. 2015, Zhou *et al*. 2014, Rana *et al*. 2015, Sabir *et al*. 2015a, Ben-Sasson *et al*. 2014, Ma *et al*. 2016, Sabir *et al*. 2015b, Nikkola *et al*. 2013, Yu *et al*. 2013). It could be seen form Table 2 that separation performance of TFC RO membrane was mainly improved through the new monomer and support developments, surface coating, grafting and nanosphere incorporation. Compared to homogeneous membrane, composite membrane could obtain the higher water flux and meanwhile kept good salt rejection as shown in Fig. 10. Nanospheres modified TFC RO membranes exhibited better salt rejection, while the water flux was relatively lower than that of other TFC RO membranes in previous literatures as shown in Fig. 10. TFC RO membranes modified by the ZnO incorporation in this study showed a higher water flux among the nanospheres modified TFC RO membranes. However, the salt rejection of the TFC RO membrane prepared in this work was moderate. This can be futher improved through the proportion optimization between the aqueous and organic phase in the presence of ZnO nanospheres. And the related work mentioned above will be studied in the future study.

3.7 Stability of separation performances

The performance stability of membranes is important during the practical operation process (Gu *et al*. 2015, Wu *et al*. 2015). In order to investigate the stability of ZnO nanospheres incorporated in the functional layer matrix, the separation performance of TFN RO membrane (RO3) were carried out through the continuous filtration of 1 $g \cdot L^{-1}$ NaCl aqueous solution at the operation pressure of 0.7 MPa. As shown in Fig. 11, the modified TFN RO membranes with 1 wt% ZnO kept a stable rejection between 91.6-95.6 % and the change of water flux was also small with a mild fluctuation (19.6-23.9 $L \cdot m^{-2} \cdot h^{-1}$) during the whole filtration process. These results suggested that the ZnO nanospheres could well be embedded in aromatic polyamide layer. This was mainly
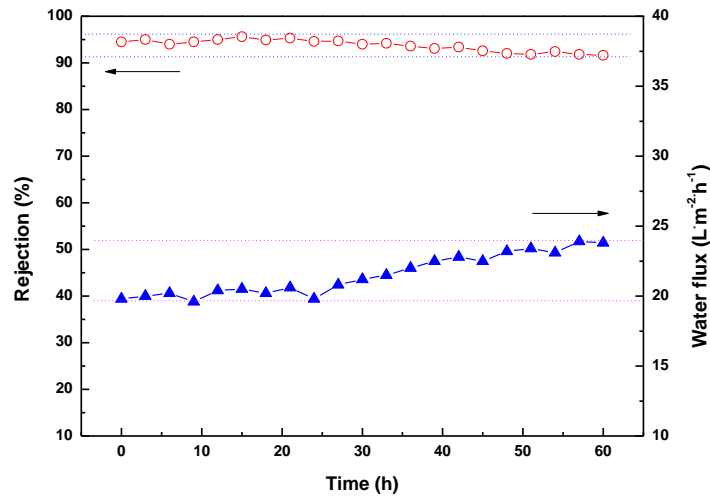
Fig. 11 The stability of separation performance of TFN RO membrane (RO3) (1 g·L^{-1} NaCl aqueous solution at 0.7 MPa, 25°C for 60 h)
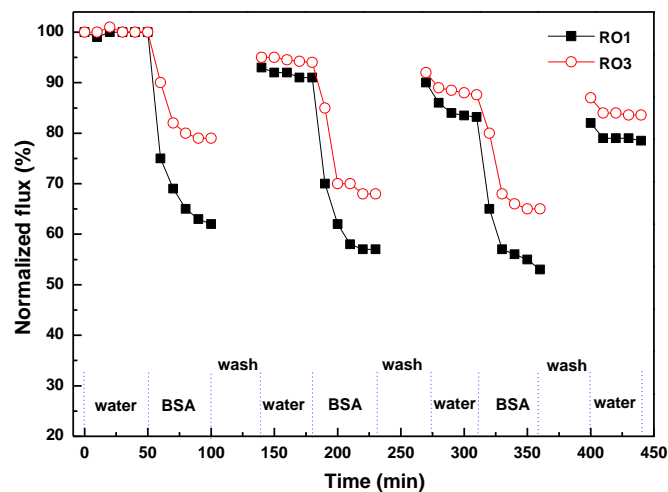

Fig. 12 Time-dependent normalized flux of the virgin and modified RO membranes

due to the interaction between C=O groups in polyamide chains and ZnO nanospheres as illustrated in Fig. 5.

3.8 Antifouling properties of the TFN RO membranes

Non-specific adsorption has an important effect on membrane fouling during varias filtration and separation process. It is appropriate to use the BSA molecules as the sticky model foulant and to evaluate non-specific adsorption (Shi *et al*. 2013). In this study, a three-cycle cross-flow protocol was carried out to evaluate the antifouling properties of the RO membrane. Fig. 12 showed the variations of normalized flux of the virgin and modified RO membranes during the
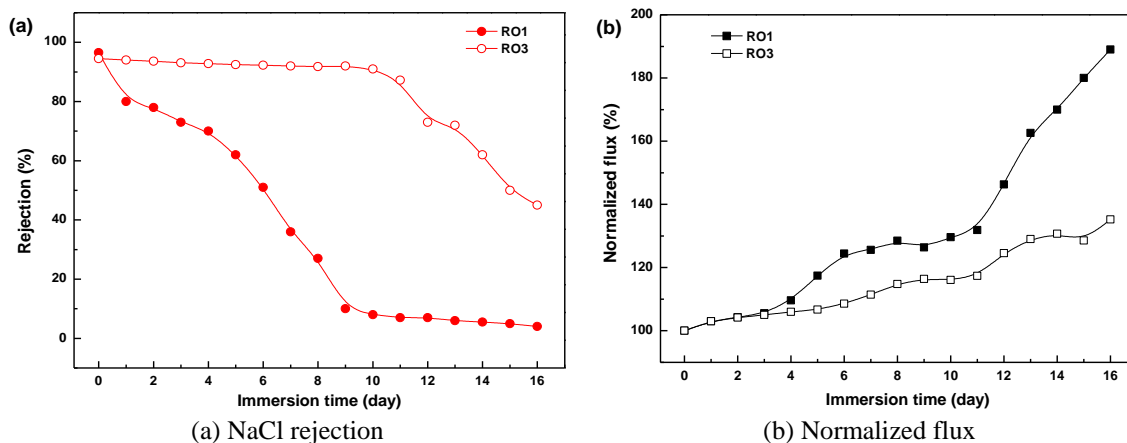
(a) NaCl rejection (b) Normalized flux

Fig. 13 Variations of different RO membrane separation performance after the exposure to 100 ppm NaClO (pH=6.5)

filtration cycles. As can be seen from Fig. 12, the TFN RO membrane had dramatically higher water flux than that of the virgin RO membrane. This indicated that the virgin RO membrane suffered the serious fouling. In addition, the flux recovery ratios of TFN RO membrane after each washing step were 95%, 92% and 87%, which were all higher than that of virgin RO membrane (93%, 90% and 82%). This result suggested that the flux recovery capacity of the modified RO membrane was stronger than that of the virgin RO membrane. The enhancement of membrane antifouling properties was mainly attributed to the improvement of membrane surface hydrophilicity.

3.9 Chlorine resistance of RO membranes

When exposed to the solution containing free chlorine, a common additive to inhibit microorganisms and to alleviate the membrane biofouling, polyamide RO membranes are prone to suffer the significant performance deterioration which limits their wide application (Han 2013, Buch *et al*. 2008). The chlorine resistance of virgin (RO1) and TFN RO membranes (RO3) was evaluated through the cross-flow filtration of 1 g·L^{-1} NaCl aqueous solution at 0.7 MPa after the immersion of NaOCl solution. The data of water flux and NaCl rejection were obtained as shown in Fig. 13. It could be seen form Fig. 13(a) that the TFN RO membrane kept high salt rejection around 90% during the first 11 days. Afterwards, an obvious decline of the salt rejection emerged when TFN membrane immersed over 11 days. By contrast, the NaCl rejection of RO1 membrane showed a continuous decline during the whole testing process. When immersed in NaClO aqueous solution for 16 days, the rejection was close to 0%. These results suggested that the chlorine resistance of polyamide RO membrane was obviously improved when incorporating a certain amount of ZnO nanospheres in the polyamide layer.

It is known that the polyamide chain was initially ruptured when the alkaline nitrogen atom in the amide bonds were attacked by the electrophilic chlorine (Konagaya and Watanabe 2000). Owing to the electron-withdrawing effect of zinc atoms on carbonyl groups of amide, the nitrogen atoms of amide would be positively charged which was shown in Fig. 13(b) and the positively charged nitrogen of amide was hard to be attacked by the electrophilic chlorine. Thus, the

halogenation of N-H groups of amide to the N-Cl groups, which controlled the cleavage of the polyamide chain, carried out slowly. Owing to the strong electron-withdrawing effect of zinc atoms on the C=O groups of amide, the nitrogen atoms combined with C=O groups of amide would be charged positively and thus the formed positively charged nitrogen of amide was hard to be attacked by the electrophilic chlorine. The continuous increasing of water flux of the TFN RO membrane was mainly ascribed to the hydrophobicity enhancement of membrane surface which was due to the halogenation of N-H groups of amide to N-Cl groups (Buch *et al.* 2008, Konagaya and Watanabe 2000). Both the hydrophobicity enhancement of membrane surface and the cleavage of polyamide chains contributed to the significant increasing of water flux of the original RO membrane.

4. Conclusions

Thin-film nanocomposite (TFN) reverse osmosis (RO) membranes were prepared through the introduction of zinc oxide nanospheres in aqueous phase during the interfacial polymerization of MPD and TMC. IR analysis verified the successful introduction of ZnO in polyamide functional layer on TFN membrane surface. Compared with original aromatic polyamide composite RO membrane, the addition of a small amount (1 wt%) of ZnO nanospheres could significantly improve RO membrane surface hydrophilicity which was mainly due to the enrichment of hydrophilic ZnO onto polyamide layer surface and the enlarged roughness of membrane surface. TFN RO membranes exhibited almost unchanged NaCl rejection and enhanced water flux when the concentration of ZnO nanosphere in the aqueous phase was lower than 1 wt%. Additionally, the separation performance of TFN RO membrane could be well maintained during the continuous testing of 60 h. The modified RO membranes also showed enchaned antifouling properties and chlorine resistance which was mainly due to the hydrophilicity improvement and the electron-withdrawing effect of zinc atoms on carbonyl groups of amide.

Acknowledgments

References

Al-Juboori, R.A. and Yusaf, T. (2012), "Biofouling in RO system: mechanisms, monitoring and controlling", *Desalinat.*, **302**, 1-23.
Azari, S., Zou, L.D. and Cornelissen, E. (2014), "Assessing the effect of surface modification of polyamide ROmembrane by l-DOPA on the short range physiochemical interactions with biopolymer fouling on the membrane", *Coll. Surf., B*, **120**, 222-228.

Bai, X., Zhang, Y.T., Wang, H., Zhang, H.Q. and Liu, J.D. (2013), "Study on the modification of positively charged composite nanofiltration membrane by TiO$_2$ nanoparticles", *Desalinat.*, **313**, 57-65.

Bao, M.R., Zhu, G.R., Wang, L., Wang, M. and Gao, C.J. (2013) , "Preparation of monodispersed spherical mesoporous nanosilica-polyamide thin film composite reverse osmosis membranes via interfacial polymerization", *Desalinat.*, **309**, 261-266.

Baroña, G.N.B., Lim, J. and Jung, B. (2012), "High performance thin film composite polyamide reverse osmosis membrane prepared via m-phenylenediamine and 2,2′-benzidinedisulfonic acid", *Desalinat.*, **291**, 69-77.

Ben-Sasson, M., Lu, X.L., Bar-Zeev, E., Zodrow, K.R., Nejati, S., Qi, G.G. and Giannelis, E.P. (2014), "In situ formation of silver nanoparticles on thin-film composite reverse osmosis membranes for biofouling mitigation", *Water Res.*, **62**, 260-270.

Bera, A., Gol, R. M., Chatterjee, S. and Jewrajka, S.K. (2015), "PEGylation and incorporation of triazine ring into thin film composite reverse osmosis membranes for enhancement of anti-organic and anti-biofouling properties", *Desalinat.*, **360**, 108-117.

Buch, P.R., Mohan, D.J. and Reddy, A.V.R. (2008), "Preparation, characterization and chlorine stability of aromatic-cycloaliphatic polyamide thin film composite membranes", *J. Membr. Sci.*, **309**, 36-44.

Cai, Y.Y., Chen, X.F., Wang, Y., Qiu, M.H. and Fan, Y.Q. (2015), "Fabrication of palladium-titania nanofiltration membranes via a colloidal sol-gel process", *Microporous Mesoporous Mater.*, **201**, 202-209.

Chae, H.R., Lee, J., Lee, C.H., Kim, I.C. and Park, P.K. (2015), "Graphene oxide-embedded thin-film composite reverse osmosis membrane with highflux, anti-biofouling, and chlorine resistance", *J. Membr. Sci.*, **483**, 128-135.

Cheng, Q.B., Zheng, Y.P., Yu, S.C., Zhu, H.W., Peng, X.Y., Liu, J., Liu, J.Q., Liu, M.H. and Gao, C.J. (2013), "Surface modification of a commercial thin-film composite polyamide reverse osmosis membrane through graft polymerization of N-isopropylacrylamide followed by acrylic acid", *J. Membr. Sci.*, **447**, 236-245.

Choi, W., Choi, J., Bang, J. and Lee, J. H. (2013), "Layer-by-layer assembly of graphene oxide nanosheets on polyamide membranes for durable reverse-osmosis applications", *ACS Appl. Mater. Interf.*, **5**, 12510-12519.

Fathizadeh, M., Aroujalian, A. and Raisi, A. (2011), "Effect of added NaX nano-zeolite into polyamide as a top thin layer of membrane on water flux and salt rejection in a reverse osmosis process", *J. Membr. Sci.*, **375**, 88-95.

Gao, X.L., Wang, H.Z., Wang, J., Huang, X. and Gao, C.J. (2013), "Surface-modified PSf UF membrane by UV-assisted graft polymerization of capsaicin derivative moiety for fouling and bacterial resistance", *J. Membr. Sci.*, **445**, 146-155.

Glater, J., Hong, S.K. and Elimelech, M. (1994), "The search for a chlorine-resistant reverse osmosis membrane", *Desalinat.*, **95**, 325-345.

Gorgojo, P. and Jimenez-Solomon, M.F. (2014), "Polyamide thin film composite membranes on cross-linked polyimide supports: Improvement of RO performance via activating solvent", *Desalinat.*, **344**, 181-188.

Gu, J.E., Lee, J.S., Park, S.H., Kim, I.T., Chan, E.P., Kwon, Y.N. and Lee, J.H. (2015), "Tailoring interlayer structure of molecular layer-by-layer assembled polyamide membranes for high separation performance", *Appl. Surf. Sci.*, **356**, 659-667.

Han, R.L. (2013), "Formation and characterization of (melamine-TMC) based thinfilm composite NF membranes for improved thermal and chlorine resistances", *J. Membr. Sci.*, **425**, 176-181.

Hong, S.P., Kim, I.C., Tak, T. and Kwon, Y.N. (2013), "Interfacially synthesized chlorine-resistant polyimide thinfilm composite (TFC) reverse osmosis (RO) membranes", *Desalinat.*, **309**, 18-26.

Hurwitz, G., Guillen, G.R. and Hoek, E.M.V. (2010) , "Probing polyamide membrane surface charge, zeta potential, wettability, and hydrophilicity with contact angle measurements", *J. Membr. Sci.*, **349**, 349-357.

Karkhanechi, H., Takagi, R. and Matsuyama, H. (2014), "Enhanced antibiofouling of RO membranes via polydopamine coating and polyzwitterion mmobilization", *Desalinat.*, **337**, 23-30.

Kim, S.G., Chun, J.H., Chun, B.H. and Kim, S.H. (2013), "Preparation, characterization and performance of

poly (aylene ether sulfone)/modified silica nanocomposite reverse osmosis membrane for seawater desalinat", *Desalinat.*, **325**, 76-83.

Konagaya, S. and Watanabe, O. (2000), "Influence of chemical structure of isophthaloyl dichloride and aliphatic, cycloaliphatic, and aromatic diamine compound polyamides on their chlorine resistance", *J. Appl. Polym. Sci.*, **76**, 201-207.

Lee, H.S., Im, S.J. and Kim, J.H. (2008), "Polyamide thin-film nanofiltration membranes containing TiO_2 nanoparticles", *Desalinat.*, **219**, 48-56.

Liu, B.C., Chen, C., Zhang, W., Crittenden, J. and Chen, Y.S. (2012), "Low-cost antifouling PVC ultrafiltration membrane fabrication with Pluronic F 127: Effect of additives on properties and performance", *Desalinat.*, **307**, 26-33.

Liu, M.H., Chen, Q., Wang, L.Z., Yu, S.C. and Gao, C.J. (2015), "Improving fouling resistance and chlorine stability of aromatic polyamide thin-film composite RO membrane by surface grafting of polyvinyl alcohol (PVA)", *Desalinat.*, **367**, 11-20.

Ma, W., Soroush, A., Luong, T.V.A., Brennan, G., Rahaman, M.S., Asadishad, B. and Tufenkji, N. (2016), "Spray- and spin-assisted layer-by-layer assembly of copper nanoparticles on thin-film composite reverse osmosis membrane for biofouling mitigation", *Water Res.*, **99**, 188-199.

Ni, L., Meng, J. Q., Li, X.G. and Zhang, Y.F. (2014), "Surface coating on the polyamide TFC RO membrane for chlorine resistance and antifouling performance improvement", *J. Membr. Sci.*, **451**, 205-215.

Nikkola, J., Liu, X., MariRaulio, Y.L., Alakomi, H.L., Wei, J. and Tang, C.Y. (2013), "Surface modification of thin film composite RO membrane for enhanced anti-biofouling performance", *J. Membr. Sci.*, **444**, 192-200.

Peyki, A., Rahimpour, A. and Jahanshahi, M. (2015), "Polyamide thin film composite membranes on cross-linked polyimide supports: Improvement of RO performance via activating solvent", *Desalinat.*, **368**, 152-158.

Peyravi, M., Jahanshahi, M., Rahimpour, A., Javadi, A. and Hajavi, S. (2014), "Novel thin film nanocomposite membranes incorporated with functionalized TiO_2 nanoparticles for organic solvent nanofiltration", *Chem. Eng. J.*, **241**, 155-166.

Pourjafar, S., Jahanshahi, M. and Rahimpour, A. (2013), "Optimization of TiO_2 modified poly(vinyl alcohol) thin film composite nanofiltration membranes using Taguchi method", *Desalinat.*, **315**, 107-114.

Rajaeian, B., Rahimpour, A., Tade, M.O. and Liu, S.M. (2013), "Fabrication and characterization of polyamide thin film nanocomposite (TFN) nanofiltration membrane impregnated with TiO_2 nanoparticles", *Desalinat.*, **313**, 176-188.

Rana, H.H., Saha, N.K. and Jewrajka, S.K. (2015), "Low fouling and improved chlorine resistant thin film composite reverse osmosis membranes by cerium(IV)/polyvinyl alcohol mediated surface modification", *Desalinat.*, **357**, 93-103.

Sabir, A., Islam, A., Shafiq, M., Shafeeq, A., Butt, M.T.Z., Ahmad, N.M., Sanaullah, K. and Jamil, T. (2015), "Novel polymer matrix composite membrane doped with fumed silica particles for reverse osmosis desalination", *Desalinat.*, **368**, 159-170.

Sabir, A., Shafiq, M., AfsheenSarwar, A., Dilshad, M.R., Shafeeq, A., Butt, M.T.Z. and Jamil, T. (2015), "Fabrication of tethered carbon nanotubes in cellulose acetate/polyethylene glycol-400 composite membranes for reverse osmosis", *Carbohydr. Polym.*, **132**, 589-597.

Safarpour, M., Khataee, A. and Vatanpour, V. (2015), "Thinfilm nanocomposite reverse osmosis membrane modified by reduced graphene oxide/TiO_2 with improved desalination performance", *J. Membr. Sci.*, **489**, 43-54.

Shi, Q., Meng, J.Q., Xu, R.S., Du, X.L. and Zhang, Y.F. (2013), "Synthesis of hydrophilic polysulfone membranes having antifouling and boron adsorption properties via blending with an amphiphilic graft glycopolymer", *J. Membr. Sci.*, **444**, 50-59.

Shin, D.H., Kim, N. and Lee, Y.T. (2011), "Modification to the polyamide TFC RO membranes for improvement of chlorine-resistance", *J. Membr. Sci.*, **376**, 302-311.

Shintani, T., Matsuyama, H. and Kurata, N. (2007), "Development of a chlorine-resistant polyamide reverse

osmosis membrane", *Desalinat.*, **207**, 340-348.

Stan, M., Popa, A., Toloman, D., Dehelean, A., Lung, I. and Katona, G. (2015), "Enhanced photocatalytic degradation properties of zinc oxide nanoparticles synthesized by using plant extracts", *Mater. Sci. Semicond. Process.*, **39**, 23-29.

Wang, C.L., Such, G.K., Widjaya, A., Lomas, H., Stevens, G., Caruso, F. and Kentish, S.E. (2012), "Click poly(ethylene glycol) multilayers on RO membranes: Fouling reduction and membrane characterization", *J. Membr. Sci.*, **409-410**, 9-15.

Wang, J., Wang, Z., Wang, J.X. and Wang, S.C. (2015), "Improving the water flux and bio-fouling resistance of reverse osmosis (RO) membrane through surface modification by zwitterionic polymer", *J. Membr. Sci.*, **493**, 188-199.

Wei, X.Y., Wang, Z., Chen, J., Wang, J.X. and Wang, S.C. (2010), "A novel method of surface modification on thin-film-composite reverse osmosis membrane by grafting hydantoin derivative", *J. Membr. Sci.*, **346**, 152-162.

Wei, X.Y., Wang, Z., Zhang, Z., Wang, J.X. and Wang, S.C. (2010), "Surface modification of commercial aromatic polyamide reverse osmosis membranes by graft polymerization of 3-allyl-5,5-dimethylhydantoin", *J. Membr. Sci.*, **351**, 222-233.

Wu, J.H., Wang, Z., Yan, W.T., Wang, Y., Wang, J.X. and Wang, S.C. (2015), "Improving the hydrophilicity and fouling resistance of RO membranes by surface immobilization of PVP based on a metal-polyphenol precursor layer", *J. Membr. Sci.*, **496**, 58-69.

Xu, J., Wang, Z., Yu, L.L., Wang, J.X. and Wang, S.C. (2013), "A novel reverse osmosis membrane with regenerable anti-biofouling and chlorine resistant properties", *J. Membr. Sci.*, **435**, 80-91.

Yamamoto, K., Ohshita, J., Mizumo, T., Kanezashi, M. and Tsuru, T. (2015), "Preparation of hydroxyl group containing bridged organosilica membranes for water desalination", *Sep. Purif. Technol.*, **156**, 396-402.

Yan, H., Miao, X.P., Xu, J., Pan, G.Y., Zhang, Y., Shi, Y.T., Guo, M. and Liu, Y.Q. (2015), "The porous structure of the fully-aromatic polyamide film in reverse osmosis membranes", *J. Membr. Sci.*, **475**, 504-510.

Yan, W.T., Wang, Z., Wu, J.H., Zhao, S., Wang, J.X. and Wang, S.C. (2016), "Enhancing the flux of brackish water TFC RO membrane by improving support surface porosity via a secondary pore-forming method", *J. Membr. Sci.*, **498**, 227-241.

Yu, S.C., Liu, M.H., Lü, Z.H., Zhou, Y. and Gao, C.J. (2009), "Aromatic-cycloaliphatic polyamide thin-film composite membrane with improved chlorine resistance prepared fromm-phenylenediamine-4-methyl and cyclohexane-1, 3, 5-tricarbonyl chloride", *J. Membr. Sci.*, **344**, 155-164.

Yu, S.C., Yao, G.H., Dong, B.Y., Zhu, H.W., Peng, X.Y., Liu, J., Liu, M.H. and Gao, C. J. (2013), "Improving fouling resistance of thin-film composite polyamide reverse osmosis membrane by coating natural hydrophilic polymer sericin", *Sep. Purif. Technol.*, **118**, 285-293.

Zhang, T.L., Zhu, C.Y., Ma, H.M., Li, R.Y., Dong, B.G., Liu, Y.F. and Li, S.Z. (2014), "Surface modification of APA-TFC membrane with quaternary ammonium cation and salicylaldehyde to improve performance", *J. Membr. Sci.*, **457**, 88-94.

Zhang, Z., Wang, Z., Wang, J.X. and Wang, S.C. (2013), "Enhancing chlorine resistances and anti-biofouling properties of commercial aromatic polyamide reverse osmosis membranes by grafting 3-allyl-5,5-dimethylhydantoin and N,N′-Methylenebis(acrylamide)", *Desalinat.*, **309**, 187-196.

Zhou, C.M., Ye, D.M., Jia, H.H., Yu, S.C., Liu, M.H. and Gao, C.J. (2014), "Surface mineralization of commercial thin-film composite polyamide membrane by depositing barium sulfate for improved reverse osmosis performance and antifouling property", *Desalinat.*, **351**, 228-235.

Zou, L., Vidalis, I., Steele, D., Michelmore, A., Low, S.P. and Verberk, J.Q.J.C. (2011), "Surface hydrophilic modification of RO membranes by plasma polymerization for low organic fouling", *J. Membr. Sci.*, **369**, 420-428.

RJ